Geomorphology 204 (2014) 302–313

Contents lists available at ScienceDirect

Geomorphology

journal homepage: www.elsevier.com/locate/geomorph

Lithalsa distribution, morphology and landscape associations in the Great Slave Lowland, Northwest Territories, Canada

Stephen A. Wolfe [a,b,*], Christopher W. Stevens [c], Adrian J. Gaanderse [b], Greg A. Oldenborger [a]

[a] Geological Survey of Canada, Natural Resources Canada, 601 Booth Street, Ottawa, ON K1A 0E8, Canada
[b] Department of Geography and Environmental Studies, Carleton University, Ottawa, Ontario, Canada
[c] SRK Consulting (US) Inc., Anchorage, AK, USA

ARTICLE INFO

Article history:
Received 30 May 2013
Received in revised form 7 August 2013
Accepted 19 August 2013
Available online 27 August 2013

Keywords:
Discontinuous permafrost
Great Slave Lowland
Lithalsa
Segregated ground ice

ABSTRACT

Lithalsas are permafrost mounds formed by ice segregation in mineral-rich soil that occur within the zone of discontinuous permafrost. Nearly 1800 lithalsas were mapped using archival aerial photographs within the Great Slave Lowland, Northwest Territories, Canada. These are up to 8 m high and several hundred meters in length and width. One lithalsa, examined by electrical resistivity and boreholes, rises 4 to 6 m above an adjacent peatland, shows clear evidence of ice-segregation at depth and ground heave of between 2.5 and 4.0 m, and is estimated to have formed within the past 700 years. Regionally, lithalsas are typically located adjacent to ponds and streams with mature forms vegetated by deciduous (birch) forest or mixed (birch and spruce) forest with a herb–shrub understory and include circular, crescentic and linear forms. They are abundant within the Lowland region, which contains widespread glaciolacustrine, lacustrine and alluvial fine-grained sediments. The lithalsas are most common within the first few tens of meters above the present level of Great Slave Lake, indicating that many are late Holocene, and some less than 1000 years, in age. A comparison with lithalsas in contemporary environments reveals that comparatively warm but extensive discontinuous permafrost, fine-grained sediments (alluvial, lacustrine, marine or glaciomarine), and available groundwater supply provide the climatic and hydro-geological parameters for the development of lithalsas in permafrost terrain. The identification of lithalsas in this region is important given their sensitivity to climate change and potential hazards to northern infrastructure upon thawing.

1. Introduction

Lithalsas, first termed as such by Harris (1993), are defined as permafrost mounds formed by ice segregation (i.e. by cryosuction without any hydrostatic pressure) within mineral soils that occur within the zone of discontinuous permafrost (Pissart et al., 1998). Previously referred to as minerogenic palsas (Åhman, 1976), cryogenic (mineral) mounds (Payette and Séguin, 1979; Lagarec, 1982) and mineral palsas (Dionne, 1978), lithalsas appear similar to palsas (Seppälä, 1986) but lack a surface cover of peat (Pissart, 2002). Lithalsas form as permafrost aggrades into the ground, causing localized ice segregation through the migration of pore water (Calmels et al., 2008a), due to temperature-gradient-induced pressure differential across a freezing front, resulting in heave of the ground surface.

Detailed studies of contemporary lithalsas have been undertaken in Yukon (Harris, 1993, 1998), and in eastern Hudson Bay of northern Quebec (Allard et al., 1996; Calmels and Allard, 2004, 2008; Calmels et al., 2008a,b; Pissart, 2010; Pissart et al., 2011), Canada (Fig. 1a), Russia (Iwahana et al., 2012) and India (Wünnemann et al., 2008). Similar contemporary features, though possibly developed from intrusive ice through high hydraulic potentials rather than ice segregation, have been noted in northern Sweden (Åckerman and Malmström, 1986; Lagerbäck and Rodhe, 1986; Westin and Zuidhoff, 2001). Rampart-like features, interpreted as thawed and collapsed remnant lithalsas, have also been identified in northern Quebec (Pissart, 2003), Belgium (Pissart, 2000), and Wales (Ross et al., 2011).

Understanding the geomorphology of lithalsas is significant for several reasons. First, lithalsas are found in ice-rich terrain (Fortier and Aubé-Maurice, 2008) that represent potential hazards to northern infrastructure upon thawing (Fortier et al., 2008). Second, lithalsas are useful geomorphic indicators of past and present conditions in permafrost environments. For example, modern and remnant lithalsas indicate potentially frost-susceptible terrain (Calmels and Allard, 2008) within present or former discontinuous permafrost conditions (Lagarec, 1982; Pissart, 2000) and decaying lithalsas may be indicators of recent climatic and ecological impacts (Vallée and Payette, 2007; Fortier and Aubé-Maurice, 2008).

Lithalsas form under a constrained set of thermal, hydrological and sedimentological conditions (An and Allard, 1995; Allard et al., 1996; Calmels et al., 2008a,b). Pissart (2003) notes that the rarity of present-

* Corresponding author at: Geological Survey of Canada, Natural Resources Canada, 601 Booth Street, Ottawa, ON K1A 0E8, Canada. Tel.: +1 613 992 7670.
E-mail address: swolfe@nrcan.gc.ca (S.A. Wolfe).

0169-555X/$ – see front matter.
http://dx.doi.org/10.1016/j.geomorph.2013.08.014

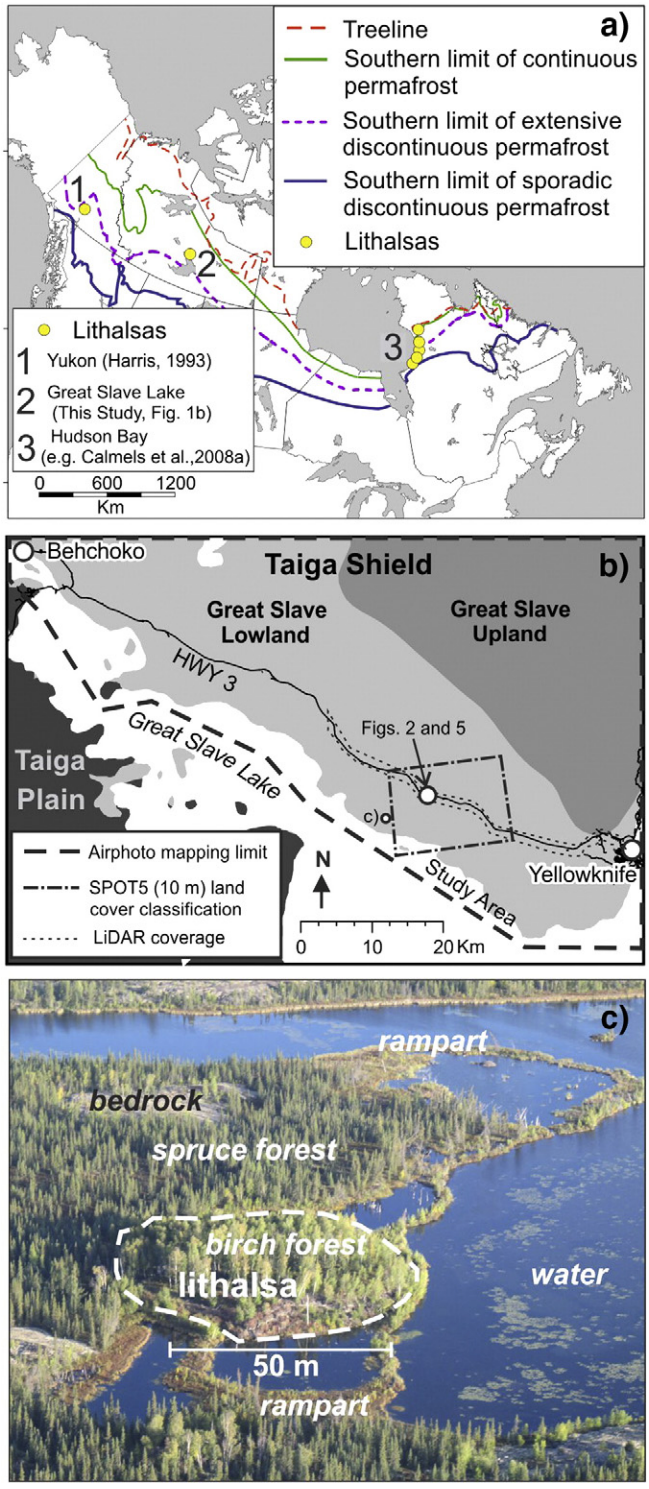

Fig. 1. Lithalsa occurrences and the study area. a) Lithalsas in Canada. Also shown is the northern limit of treeline, and southern limits of continuous, extensive discontinuous, and sporadic discontinuous permafrost from Heginbottom et al. (1995). b) Boundary of study area and the extent of imagery coverage in the Great Slave Lowland, as defined by the Ecosystem Classification Group (2008). c) Example of a lithalsa within the study area (outlined in white dashed line) at 62°32′40″N; 115°00′38″W.

day and remnant lithalsas may be related, in part, to the specific climatic conditions needed to support them. Specifically, Pissart (2000, 2002) suggests that lithalsas are restricted to the discontinuous permafrost zone, close to the treeline where mean annual air temperature ranges from −4 °C to −6 °C and where the annual temperature of the warmest month is between +9 °C and +11.5 °C. He further hypothesizes that probable locations for lithalsas in North America, where the tree line adjoins the discontinuous permafrost limit, include northern Quebec and north of Great Slave Lake, Canada, and western Alaska in the United States (Pissart, 2002).

In this paper, we test Pissart's hypothesis regarding the northern Great Slave Lake region, Northwest Territories, Canada (Fig. 1a). We examine the internal stratigraphy of a permafrost mound in the widespread discontinuous permafrost terrain of the Great Slave Lowland. We further examine the morphology, distribution and landscape association of nearly 1800 similar features in the region. Our results are discussed in the context of landscape associations (surficial geology, hydrology and land cover) and previous studies in order to improve the knowledge and constraints on the extent of lithalsas in discontinuous permafrost.

2. Study area

The Great Slave Lowland is located along the northwestern shore of Great Slave Lake, Northwest Territories, Canada (Fig. 1a, b). This 6000 km^2 land area occupies poorly-drained low relief terrain characterized by numerous water bodies separated by fens, peatlands, mixed woodlands, white birch (*Betula papyrifera*) and black spruce (*Picea mariana*) forests and bedrock outcrops. The region is bordered to the south by the North Arm of Great Slave Lake and to the north by the Great Slave Upland of higher relief and bedrock occurrence. The region was glaciated until about 13,000 cal BP (Dyke et al., 2003). With the retreat of glacial ice, glacial Lake McConnell and, subsequently, Great Slave Lake inundated the Lowland (Lemmen et al., 1994; Smith, 1994). Lacustrine silts and clays deposited into these former water bodies constitute the majority of the surficial sediments occurring across the Lowland (Stevens et al., 2012). The regional surface hydrology trends from north-to-south towards Great Slave Lake, but the fine-grained sediments and a low topographic gradient contribute to poor hydrological drainage across the area. Consequently, fire frequency and burn extent is low in the Great Slave Lowland in contrast to the better-drained Upland.

The continental climate of the Lowland is characterized by a mean annual air temperature of −4.6 °C and a mean total precipitation of 281 mm, with 42% falling as snow (Environment Canada, 2012 — climate normals from 1971 to 2000). Since the 1940s, annual mean air temperature has risen by about 0.3 °C per decade (Hoeve et al., 2004; Riseborough et al., 2012). Permafrost is extensively discontinuous (50–90%) in lateral extent, with an estimated medium to low visible ground ice content (20 to <10%) in the upper 10 to 20 m (Heginbottom et al., 1995). Permafrost temperatures beneath undisturbed terrain are generally warmer than −2 °C (Karunaratne et al., 2008) and permafrost is less than 50 m thick near Yellowknife (Brown, 1973).

To date, lithalsas and similar periglacial features such as palsas, pingos, or seasonal frost mounds, have not been recognized within the Great Slave Lowland. Nevertheless, numerous mounds are apparent throughout the region (Fig. 1c). These features are several meters high and tens to hundreds of meters across, typically devoid of peat and vegetated by deciduous or mixed forest, and commonly border water bodies. In addition, ramparts are also common, and resemble those interpreted as remnant collapsed lithalsas in Belgium (Pissart, 2000) and as decayed lithalsas in northern Quebec (Calmels et al., 2008a; Fortier and Aubé-Maurice, 2008).

In this study, we first examine the internal stratigraphy of one of these permafrost mounds at a field site (62°32′N; 114°58′W; Fig. 2), using electrical resistivity and borehole analysis. With results supporting a lithalsa hypothesis, we then examine the topographic expression and morphometric characteristics of eleven other potential lithalsas in the local study area using light detection and ranging

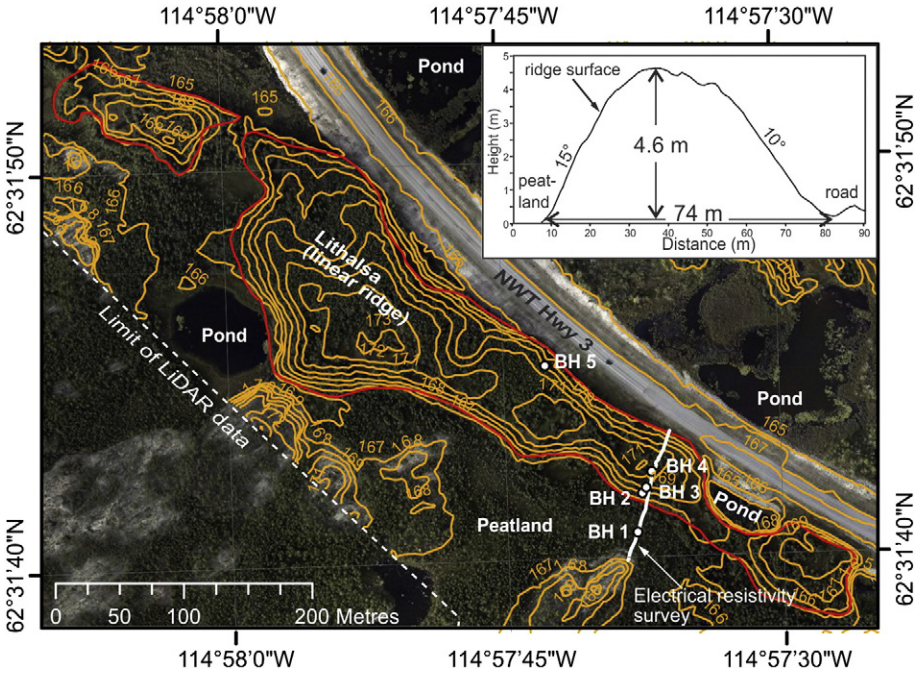

Fig. 2. Color orthophoto and 1 m lidar-derived elevation contours (shown in orange) of the linear ridge field site (limit of lithalsa shown in red) with locations of electrical resistivity survey and boreholes. Inset depicts elevation cross-section across the ridge.

(lidar) and color orthorectified aerial photographs. We then map the broader distribution of lithalsas across a 3680 km^2 area of Great Slave Lowland and Upland using archival aerial photographs, and examine their association with elevation, surficial geology, surface hydrology and land cover. Our discussion includes a comparison of contemporary lithalsas in discontinuous permafrost environments aimed at developing an improved understanding of the environmental constraints on these features.

3. Methods

3.1. Stratigraphic field and laboratory methods

A galvanic electrical resistivity survey was conducted at a field site (Figs. 1b and 2) across a peatland and elevated terrain identified as a permafrost mound, to determine the approximate depths to bedrock and the presence of ice-bonded, ice-bearing and unfrozen sediments (see Oldenborger, 2012; Oldenborger et al., 2012 for methods).

Additional stratigraphy was obtained from frozen sediment in five cores recovered with a Cold Regions Research Engineering Laboratories (CRREL) coring barrel powered by a 2-person handheld Stihl® engine. To assess the lithalsa hypothesis, sediments were analyzed for particle-size, frozen bulk density, gravimetric moisture and visible ice content, with organic material collected for AMS dating.

Other field methods included ground-level observations and aerial surveys to acquire low-level oblique aerial photographs of other potential lithalsas, and to document broader landscape associations with elevation, surficial geology, hydrology and land cover.

3.2. Lidar-derived morphometric analysis

Lidar data were used to identify lithalsa terrain for detailed field investigations and to examine their topographic and morphometric attributes. Lidar data were acquired in the near-infrared wavelength (maximum pulse rate of 150 kHZ) from a Piper Navajo fixed wing aircraft using a Leica ALS50-II with MPiA, along a 40 km linear transect (Fig. 1b) on August 22 and 24, 2010 by McElhanney Consulting Services Ltd. Flight lines were flown with 30% overlap at an altitude of 1506 m asl, resulting in a 30° field of view and a maximum swath width of 723 m. The average bare earth point cloud density for this dataset was determined to be 2.24 pts m^{-2} (McElhanney Consulting Services Ltd. pers. comm.). Colored aerial photographs were also acquired during the lidar survey using a Trimble RolleiMetric AIC P65+ with a 60-megapixel sensor to produce 20-cm resolution true-color RGB photographs. Orthorectification of the aerial photographs was performed by McElhanney Consulting Services Ltd.

The vertical accuracy of the lidar data was assessed using the American Society for Photogrammetry and Remote Sensing guidelines (Shan and Toth, 2008). The average discrepancy between the lidar and RTK GPS measurements was reported to be −0.03 cm, with a range of −11.5 to +15.2 cm (McElhanney Consulting Services Ltd. pers. comm.).

A 1 m bare-earth digital elevation model (DEM) was derived from the lidar point cloud data to determine morphometric attributes of individual lithalsas. Lithalsa width (w) was calculated perpendicular to the long axis of linear features and transverse to the center of circular features (Fig. 3), as:

$$w = d_1 - d_2 \quad (1)$$

where d_1 and d_2 are points along the elevation profile that define the break in slope between the lithalsa and the surrounding terrain, and their separation distance defines the cross-sectional width. Lithalsa height (h) was calculated as

$$h = Z_{max} - \left(z_1 - \left(\frac{z_1 - z_2}{2}\right)\right) \quad (2)$$

where z_1 and z_2 are the elevations at distances d_1 and d_2, and Z_{max} is the maximum height along the elevation profile. These two calculations were used to determine the height to width ratio.

3.3. Stereo aerial photograph and satellite image interpretation

Lithalsas were mapped over 3680 km^2 using monochromatic 1:60,000 scale aerial photographs, acquired between 1978 and 1980.

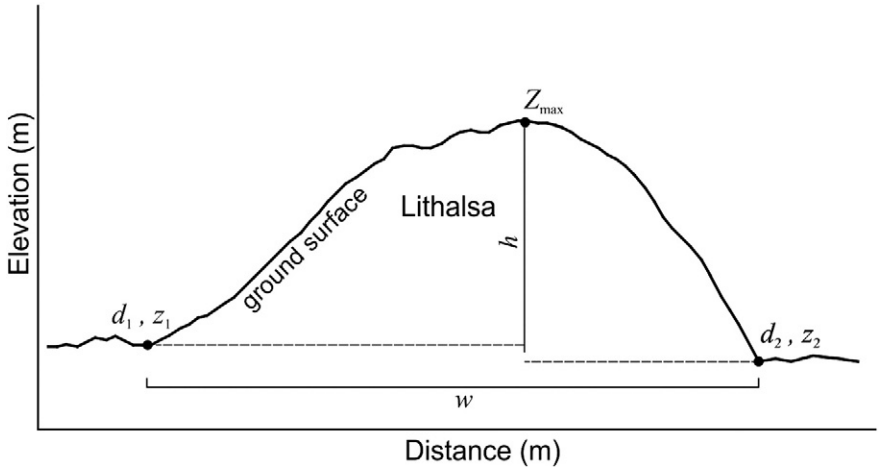

Fig. 3. Schematic diagram illustrating the location of distance and elevation points used to determine lithalsa horizontal and vertical dimensions (see Eqs. (1) and (2)).

The mapping area extends across one-third of the Great Slave Lowland and a portion of the Upland terrain (Fig. 1b).

Lithalsas were manually identified from the surrounding terrain in the monochromatic aerial photographs on the basis of image tone and texture, and 3-dimensional topographic effects observed in stereo view, using lithalsas detected from lidar bare-earth topography and color orthorectified aerial photographs as initial training areas. Lithalsas were characterized in stereo-pair aerial photographs as locally elevated terrain with medium-to-dark tone and a smooth texture in contrast to bedrock outcrops with light tone and rough texture. This image analysis was limited by the scale of the aerial photographs, and likely underestimated the total number of features present in the map area due to the inability to detect smaller features, typically less than 15 meters wide in this case, with low topographic expression. However, the data produced likely reflect the general distribution of features across the landscape.

The location of each lithalsa was digitized as a point feature overlying a georeferenced LANDSAT 7 image. WorldView-2 and GeoEye1 satellite imagery (50-cm spatial resolution) were utilized in the digitization process for improved spatial accuracy. The association between lithalsas and land cover was made using vegetation and terrain classifications derived from normalized peak-of-season 10-m resolution SPOT-5 imagery acquired between 2007 and 2010, as described by Olthof et al. (2012, 2013), acquired over a portion of the study area (Fig. 1b).

4. Results

4.1. Field site stratigraphy

Northwest Territories Highway 3 traverses the Great Slave Lowland west of Yellowknife. Unconsolidated sediments throughout this area consist of silts and clays, deposited in former glaciolacustrine and lacustrine environments. These surficial sediments typically infill bedrock valleys and depressions in the Lowland, resulting in a relatively level topographic expression with undulating bedrock outcrops. However, ridges up to 8 m high and several hundred in length are noted at various locations along the highway. At one location (62°32′N; 114°58′W) a 600 m long ridge, rising up to 6 m above the surrounding terrain and up to 130 m wide, resides along the south side of the highway (Fig. 2). The ridge abuts a peatland along most of its southern side and a pond along the northern side; noting the highway at this location is constructed across the pond (Oldenborger et al., 2012). The peatland is vegetated with black spruce and an understory of Labrador tea (*Rhododendron groenlandicum*) and moss, underlain by about 90 cm of peat. In contrast, the ridge is vegetated with white birch and white spruce (*Picea glauca*) forest and an understory of herbs and shrubs, including fireweed (*Epilobium angustifolium*) and rose (*Rosa* spp.), with a thin organic cover of 10 cm or less.

An electrical resistivity survey was conducted across this ridge, where there is about a 4 m height difference between the peatland and the top of the ridge. The survey extended from exposed bedrock at the southern end, across the peatland and ridge, to the highway embankment at the northern end (Figs. 2 and 4a). The exposed, highly resistive bedrock is interpreted as extending below the peatland in the survey. A borehole drilled in the peatland about 30 m off the survey line and without core recovery encountered bedrock at a depth of about 9 m. A low resistivity layer, observed at the surface along the entire geophysical survey is thinnest over the peatland, thicker across the ridge, and thickest at both the southern and northern margins of the ridge adjacent to the peatland and road embankment (Fig. 2). Probing of the ground confirmed this layer to be unfrozen; corresponding to the active layer (i.e. seasonally frozen and thawed surface layer of ground), which was approximately 40 cm thick in the peatland and approximately 180 cm thick on the ridge. At either edge of the ridge, low resistivity anomalies extending to about 10 m depth are interpreted as probable taliks (i.e. perennially unfrozen ground). These areas correspond to the highway right-of-way, on the north side of the ridge, and an area of shallow perennial ponding on the south side.

Other considerable differences in resistivity are observed beneath the ridge and the peatland (Fig. 4a). For the ridge, a thick, highly resistive zone is encountered below the low resistivity surface layer, at about 5 m depth. In contrast, for the peatland, a relatively thin, moderately resistive zone is encountered below the active layer, which is underlain by a less resistive zone at about 5 m and higher resistive bedrock at about 13 m. Soils beneath the active layer on the ridge are interpreted to be ice-bonded permafrost, with ice-rich permafrost below 5 m at depth, based upon the high resistivity, as similarly noted by Fortier et al. (2008). In contrast, the peatland is inferred to have only a thin layer of ice-bonded permafrost underlain by a layer containing high unfrozen water content, based on the lower resistivity comparable to the active layer and interpreted taliks.

Five boreholes were drilled on the ridge and peatland to verify the electrical resistivity results and provide additional stratigraphy for interpretation (Fig. 4b). All boreholes encountered similar sediment stratigraphy, with clayey-silt and silty-sand units underlain by a clay unit at depths of 4 m (BH-1) to 6 m (BH-5) below the surface. The clay unit is interpreted as glaciolacustrine sediment (i.e. from Glacial Lake McConnell), as evident from small isolated dropstones and absence of detrital organic material. Sediments overlying the clay are interpreted as lacustrine and alluvial sediments related to progressive Holocene drawdown of Great Slave Lake. AMS radiocarbon analysis from a sample at 62 cm depth from the base of the organic deposits in BH-1 in the

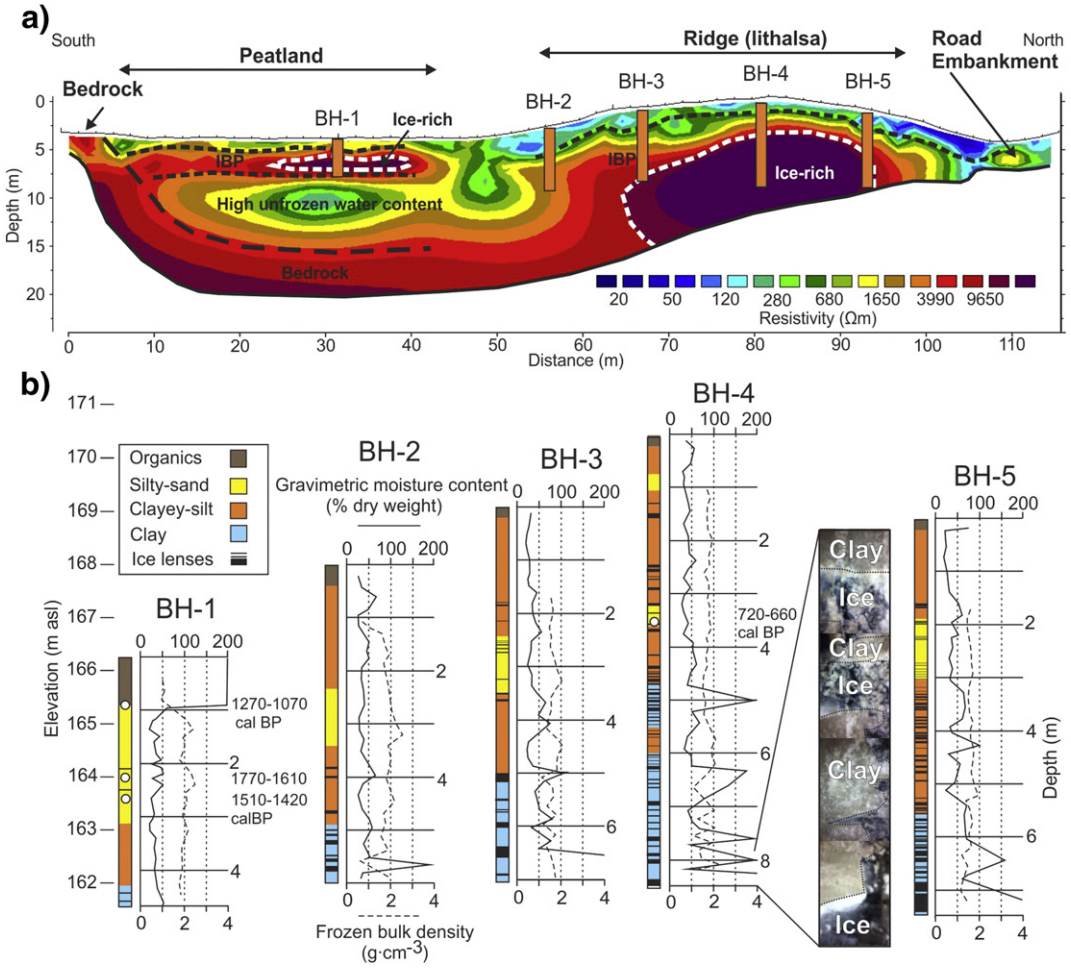

Fig. 4. Electrical resistivity model and borehole stratigraphy across the peatland and the ridge at the linear ridge lithalsa field site (Fig. 2). a) Interpreted electrical resistivity model indicating ice-rich permafrost, ice-bonded permafrost (IBP), and ground with high unfrozen water content. b) Stratigraphy, AMS ages, gravimetric moisture content and bulk density from boreholes.

peatland returned an age at 2σ standard deviation of 1270–1070 cal BP (Beta-309231; 1240 ± 30 BP), signifying terrestrial exposure and permafrost aggradation into the peatland after this time. Detrital organics (burned wood) from a silty-sand unit below the peat at 220 cm and 255 cm, interpreted as alluvial sediment, dated to ca. 1700 and 1450 cal BP (Beta 317798; 1770 ± 30 BP and 317799; 1570 ± 30 BP) confirming late Holocene sedimentation. Most significantly, however, was an AMS age of 720–660 cal BP (Beta-331114; 740 ± 30 BP) recovered from detrital organics at 3.5 m depth in silty-sand sediment in BH-4. This age signifies that lacustrine or alluvial deposition continued here until at least 700 years ago, and that subsequent terrestrial exposure and permafrost aggradation within the ridge must have occurred within the past 700 years.

Gravimetric moisture contents and bulk densities (Fig. 4b) reveal significant differences between units, reflecting an increase in the volume of ground ice in clays at lower depths. Moisture contents in the overlying silty-sand and sandy-silt units generally range between 30% and 60% (mass water/mass dry soil) and frozen bulk densities between 1.5 and 2.4 g cm^{-3}, but are highly variable in the clay unit due to the presence of ice layers, with moisture contents exceeding 200% (mass water/mass dry soil) and bulk densities near 1.0 g cm^{-3}. Visible ice, on the order of 50% by volume, occurs in the form of horizontal and vertical lenses up to 10 cm thick (Fig. 4b). Cryostructures, including suspended clay inclusions and bubble-rich ice at the clay–ice contacts, indicate segregated ice formed via cryosuction and the migration of pore water as permafrost aggraded into the sediments (Calmels and Allard, 2008; Calmels et al., 2008a). In addition, stiff clay layers between these ice lenses with high bulk densities (up to 2.0 g cm^{-3} in BH-4) are further indicative of clay consolidation resulting from cryosuction during ice lens formation.

Given the observed stratigraphy, there is likely some geological component of the electrical interface at approximately 5 m depth under the peatland, as clay is expected to be more conductive than silt/sand. However, the contrast is too great to be attributable entirely to a silt/clay transition and the interpretation of ice-bonded permafrost over high unfrozen water content stands. Under the ridge, the active layer and ice dominate the electrical signature and the stratigraphic contact is only observed indirectly as corresponding to ice-bonded permafrost.

Given the lack of sandy sediments here and throughout the lowlands, it is unlikely that this or any of the other permafrost mounds represent a pingo (Mackay, 1998). Furthermore, the lack of peat cover is inconsistent with a palsa (Pissart, 2002). Lastly, the absence of season change in surface morphology is inconsistent with seasonal frost mounds (Nelson et al., 1992). However, the geophysical and stratigraphic observations support the hypothesis that the ridge is a lithalsa, and that it likely formed within the past 700 years as permafrost aggraded into underlying fine-grained sediments. A 5.0 m difference in elevation between the top of the sediment on the ridge and the top of sediment in the surrounding peatland is postulated as resulting from differential ground heave associated with the additional volume of ice beneath the ridge, though the ground heave is likely offset to some degree by cryogenic consolidation of the mineral soil. An

assessment of the excess ground ice in the ridge can also be made by examining the difference in elevation at the contact with the underlying clay unit, assuming that the original contact was horizontal and noting that it rises in elevation beneath the ridge in comparison to the peatland, likely due to heave from ice-lens formation; this difference is about 4.0 m.

4.2. Topographic expression and morphometric characteristics

Fig. 5 illustrates plan views and cross-sections of two other lithalsa forms recognized from lidar data and color orthophotographs. The lithalsas are identifiable as vegetated ridges or mounds that are clearly distinguished from bedrock outcrops on the color images. Typical forms in the area include circular lithalsas that are roughly axis-symmetrical in plan view and conical in form (Fig. 5a). Other lithalsas are ridge-like, including crescentic lithalsas that are curvilinear in plan view (Fig. 5b), and linear lithalsas that are typically elongate and asymmetrical in plan view as noted at the field site (Fig. 2).

The side slopes of the lithalsas commonly range from 5 to 15° at the peripheral edge adjacent to land. Where the lithalsas border water bodies (lithalsa–pond transitions), side slopes are more commonly 15 to 20°, and may represent evidence of historical degradation. Lithalsas with a truncated cross-sectional profile are also characterized by side slopes ranging from 20 to 30°, likely related to over-steepened slopes caused by slumping of sediment into the adjacent ponds and thaw consolidation of underlying ice-rich permafrost, and indicative of lithalsa degradation (Fig. 5a).

A statistically significant linear relation exists between lithalsa height and width in this area (Fig. 6). Following a functional fit (Mark and Church, 1977), a 1 m increase in lithalsa height is accompanied by about 15 m of lateral growth. The lateral growth is interpreted to result from the change in ground ice volume over time as segregated ice develops in the lithalsa with both vertical and lateral permafrost aggradation (Pissart et al., 2011). Dilation cracks were observed at the surface both parallel and orthogonal to the long axis of the linear ridge at the field site, further supporting this interpretation. This linear relation could further be used to predict lithalsa height based on measured widths from aerial photographs or satellite imagery.

4.3. Spatial distribution of lithalsas and landscape associations

4.3.1. Spatial distribution of lithalsas

The spatial distribution of lithalsas manually identified from the monochromatic 1:60,000 scale aerial photographs is shown in Fig. 7a. Of the 1777 individual lithalsas, 1737 (98%) are located within the Great Slave Lowland below an elevation of 205 m asl. Another 40 lithalsas (2%) occur within a portion of the Great Slave Upland. The spatial density of lithalsas across the Lowland is up to 10 per km^2. Lithalsa distribution is positivity skewed, however, towards lower elevations close to the present-day level of Great Slave Lake (~156 m asl) and declines at higher elevations. Approximately 70% of all mapped lithalsas occur within 15 m of the modern level of Great Slave Lake, which is disproportionate to the land area (40%) represented by these elevations.

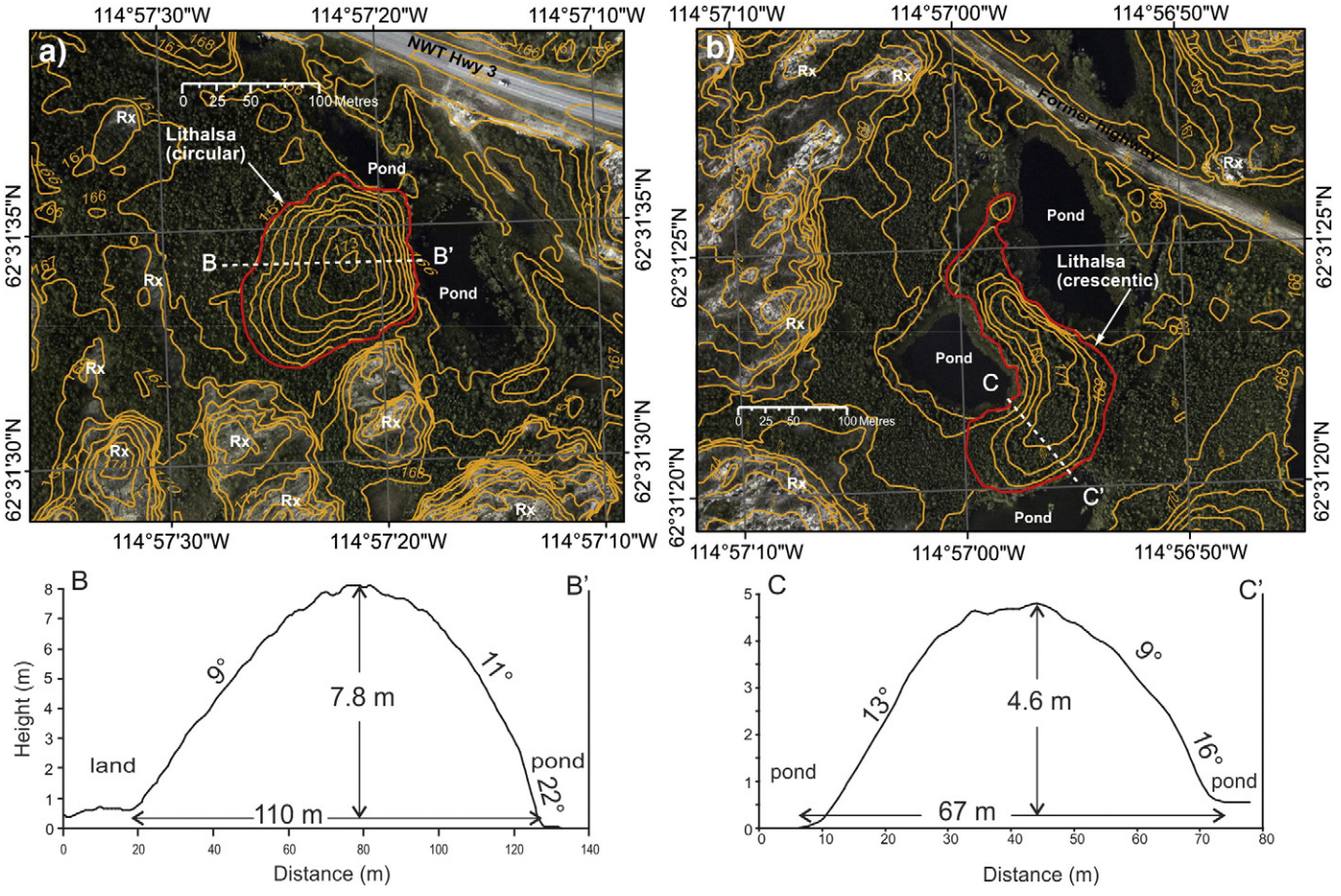

Fig. 5. Lithalsas with a) circular morphology and b) crescentic morphology (shown in red lines) in the study area recognized from color orthophotos with 1 m lidar-derived elevation contours (orange lines). Also shown are elevation cross-sections across the lithalsas. Note the hill-shaped lithalsas exhibit a smooth vegetated surface in contrast to rough bedrock (Rx) outcrops, and also the close proximity of the lithalsas to water bodies (ponds). Lithalsas in a) and b) are 200 and 600 m southeast of the lithalsa in Fig. 2, respectively.

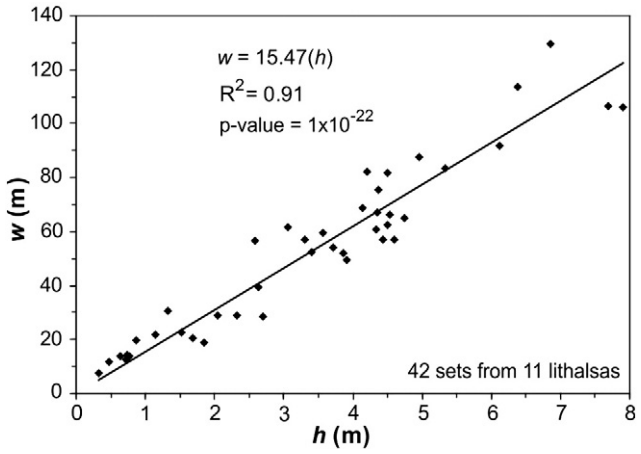

Fig. 6. Functional relation of lithalsa width (w) to height (h). Dimensions were calculated from Eqs. (1) and (2) using lidar data acquired along various cross-sections located on eleven individual lithalsas ($n = 42$).

Similarly, approximately 30% of lithalsas occur within 5 m of the modern lake level (Fig. 7 inset).

4.3.2. Surficial geology

The regional occurrence of lithalsas correlates with the mapped distribution of glaciolacustrine silt and clay (Fig. 8), with nearly 99% of all lithalsas occurring in areas of glaciolacustrine silt and clay, wetlands or water. Silt and clay covers nearly 70% of the mapped area below an elevation of 205 m asl within the Great Slave Lowland. Above this elevation the terrain is nearly devoid of lithalsas, and consists predominately of bedrock with isolated glaciolacustrine and glaciofluvial deposits. It may be inferred from this comparison that lithalsa formation in the region requires fine-grained silts and clays.

4.3.3. Surface hydrology

Fig. 9 shows additional examples of lithalsas, illustrating some of their morphologies and association with surficial sediment, water bodies and vegetation cover. Lithalsas within the mapped area mainly occur adjacent to ponds, rivers and streams (Figs. 2 and 9). Overall, the highest occurrence of lithalsas is within poorly-drained low-lying valleys defined by bedrock faults that, in part, control the flow direction of surface hydrology and the location of lakes and ponds. Lithalsas are typically absent across well-drained terrain in both the Great Slave Upland (Fig. 7a) and localized regions of the Lowland (Fig. 7b). The hydrological control on lithalsa distribution is evident in Fig. 7b where these features are concentrated within stream and river flow networks, along which lakes and ponds occur, and are generally absent on upland surfaces. Nearer to the present Great Slave Lake shoreline, lithalsas tend to be concentrated near the mouth of modern stream outlets and within larger embayments. It is likely that the underlying fine-grained alluvial and lacustrine sediments are thickest here, accounting, in part, for the higher concentration of lithalsas in these areas.

4.3.4. Land cover

Table 1 summarizes the land cover associated with 175 lithalsas in the Great Slave Lowland covered by the SPOT5 land cover classification (Fig. 1b). The absence of forest fires in this region suggests that land cover has been historically unaffected by these major disturbance factors. Lithalsas are most commonly associated with medium to high density deciduous (birch) and mixed (birch–spruce) forests and medium to high density coniferous (spruce) forests. Independent of forest density, approximately 70% of the lithalsas are associated with deciduous forests and mixed deciduous–coniferous forests. About 24% of lithalsas are vegetated with coniferous (spruce) forests, typically of low to medium density. An additional 6% of lithalsas occupy spruce–lichen wetlands (i.e. peatlands) and wetland/fen environments. It should be noted that the actual percentage of lithalsas occupied by each land cover type may be somewhat influenced by a mapping bias towards larger lithalsas. As a result, the percentages only accurately reflect the portion of larger lithalsas associated with the different land cover types.

Fig. 9 illustrates field photographic evidence of vegetation types associated with different sized lithalsas. Smaller lithalsas are observed to occupy wetland fens to spruce wetland environments, forming narrow ribbon-like "rampart" features within and adjacent to water bodies (Fig. 9a). These forms contrast with larger lithalsas vegetated with deciduous birch, herb understory (fireweed) and white spruce (Fig. 9b–d). In some instances, these ramparts may represent remnant collapsed lithalsas and in other cases possibly incipient lithalsa forms. Collapsed (i.e. thawed) lithalsas with circular remnant ramparts are well-recognized elsewhere (Pissart, 2003; Calmels et al., 2008a) and likely occur in the Great Slave Lowland area as well. Consolidation of clay sediments due to cryosuction results in a situation where, after the permafrost thaws, a depression several meters deep forms, leaving only a remnant ringed-shaped rampart around a thermokarst pond (Fortier and Aubé-Maurice, 2008). Photographic and field evidence indicates that these features also undergo a vegetation succession as they develop, as was similarly noted for lithalsas in Yukon, Canada, by Harris (1993), thus supporting the hypothesis of incipient lithalsa forms in many cases. Incipient lithalsas in the Great Slave Lowland area are dominated by wetland shrub vegetation. An increase in lithalsa height is accompanied by birch and white spruce, which require relatively well-drained surface conditions. Whereas a detailed analysis of these rampart forms has not been undertaken at present, an examination of rampart vegetation and soil associations could further assist in distinguishing their origins.

5. Discussion

5.1. Morphology and settings of contemporary lithalsas

Table 2 summarizes the morphology and climatic, stratigraphic, geomorphic and ecological conditions associated with lithalsas in contemporary permafrost environments.

Morphologically, the northern Great Slave Lake lithalsas are similar to those in other regions and include circular, crescentic and linear forms. Circular lithalsas are common in northern Quebec, and also occur in Yukon and the Tso Kar Basin, India, where crescentic and linear forms (respectively) also occur. In contrast, lithalsas of the Akkol Valley, the Russian Altai Mountains, are typically linear and adjacent to individual lakes. We hypothesize that the variation in lithalsa form is related, in part, to the spatial supply of groundwater for ice-segregation. In Canada, contemporary lithalsas are found in close proximity to water sources within modern stream valleys and shorelines, and elsewhere are found adjacent to ponds or within large lake basins. Circular lithalsas may form on relatively uniform surfaces such as broad lake basins or valleys and marine lowlands where there may be a uniform subsurface water supply. In contrast, lithalsas with distinctively linear and crescentic forms appear indicative of an asymmetric water supply as these forms more commonly occur adjacent to ponds or streams. The spatial distribution of water supply affects the abundance of water for ice-lens formation, and thus will likely affect the size and orientation of ice lenses and cryostructures at depth. This, in turn, may affect the morphological relief and cross-sectional symmetry (or, specifically, asymmetry) of lithalsas. As noted in the Great Slave Lowland, the variable distribution of surficial sediment and undulating bedrock outcrops probably also plays a role in water availability and the comparatively complex morphology of lithalsas.

Great Slave lithalsas are comparable in height (up to 8 m) to other lithalsas, but tend to be wider and longer than most others. Lithalsa

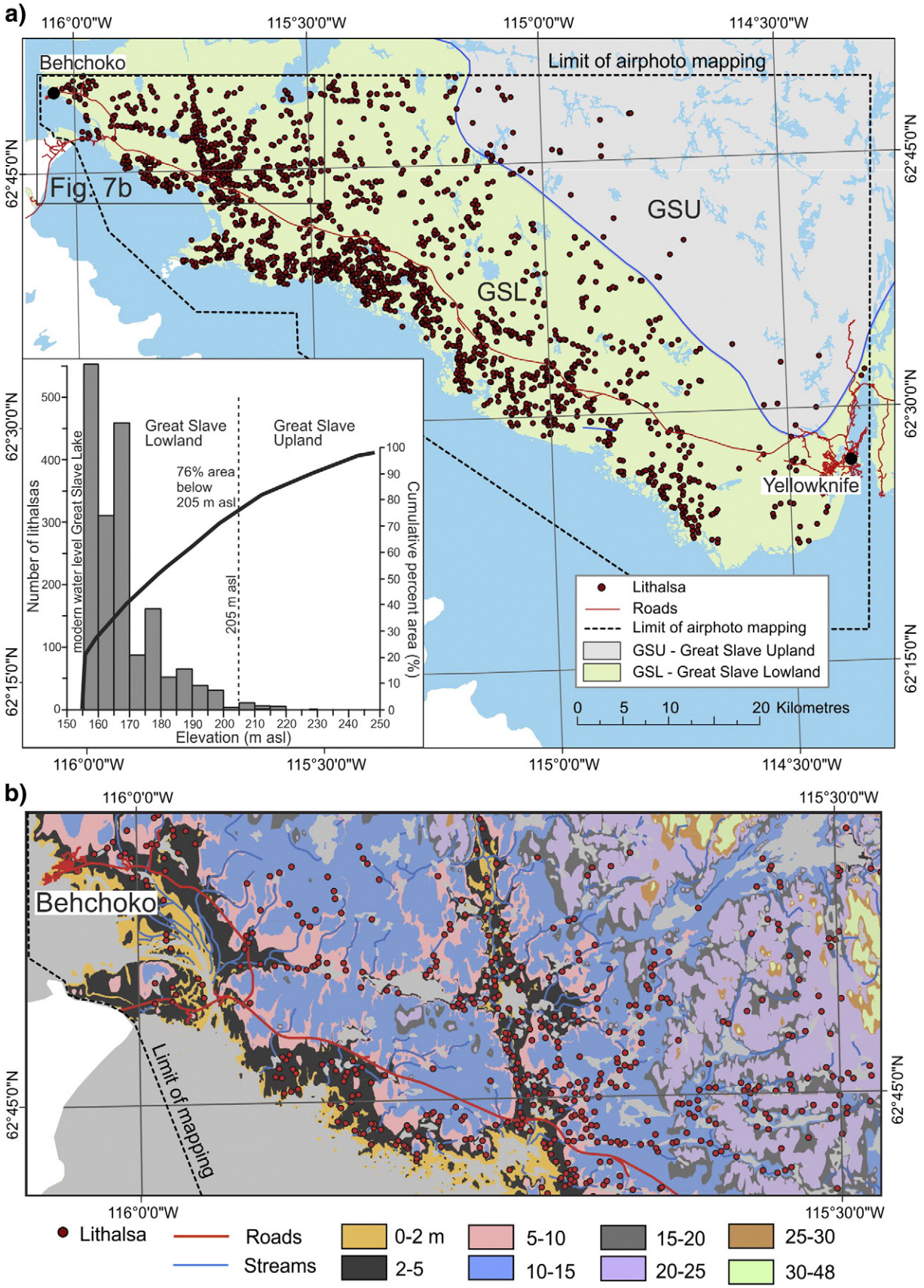

Fig. 7. Regional lithalsa distribution. a) Distribution of 1777 lithalsas identified within the limit of mapping in the Great Slave Upland (GSU) and Great Slave Lowland (GSL) based on aerial photograph interpretation. Inset depicts histogram of number of lithalsas at 5 m intervals above modern level of Great Slave Lake (156 m asl) and the hypsometric curve of elevation within the limit of mapping. b) Detailed map of lithalsa distribution in relation to elevation above Great Slave Lake. Note abundance of lithalsas within 5 m above modern lake level, and the association between lithalsas and stream channels. Color coded elevations are based on the 1:50,000 scale Canadian Digital Elevation Data (CDED).

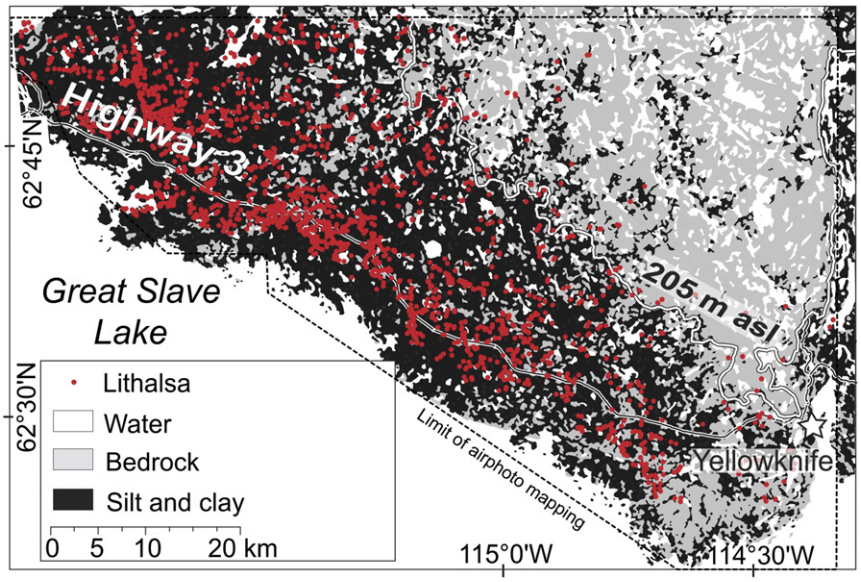

Fig. 8. Simplified surficial sediment map (Stevens et al., 2012) showing distribution of lithalsas, silt and clay sediments and exposed bedrock in the study area.

height may be controlled by several factors including thickness of frost susceptible sediment, water supply and availability, and the thickness (i.e. depth) of permafrost. In the Great Slave region, thickness of frost-susceptible sediment and depth to bedrock are likely the main factors controlling the maximum height of lithalsas, whereas water availability may play an important role in the height-to-width ratio and the overall length. Notably, the volume of ground ice at depth within the Great Slave lithalsas (~50%) is comparable to other lithalsas, suggesting that

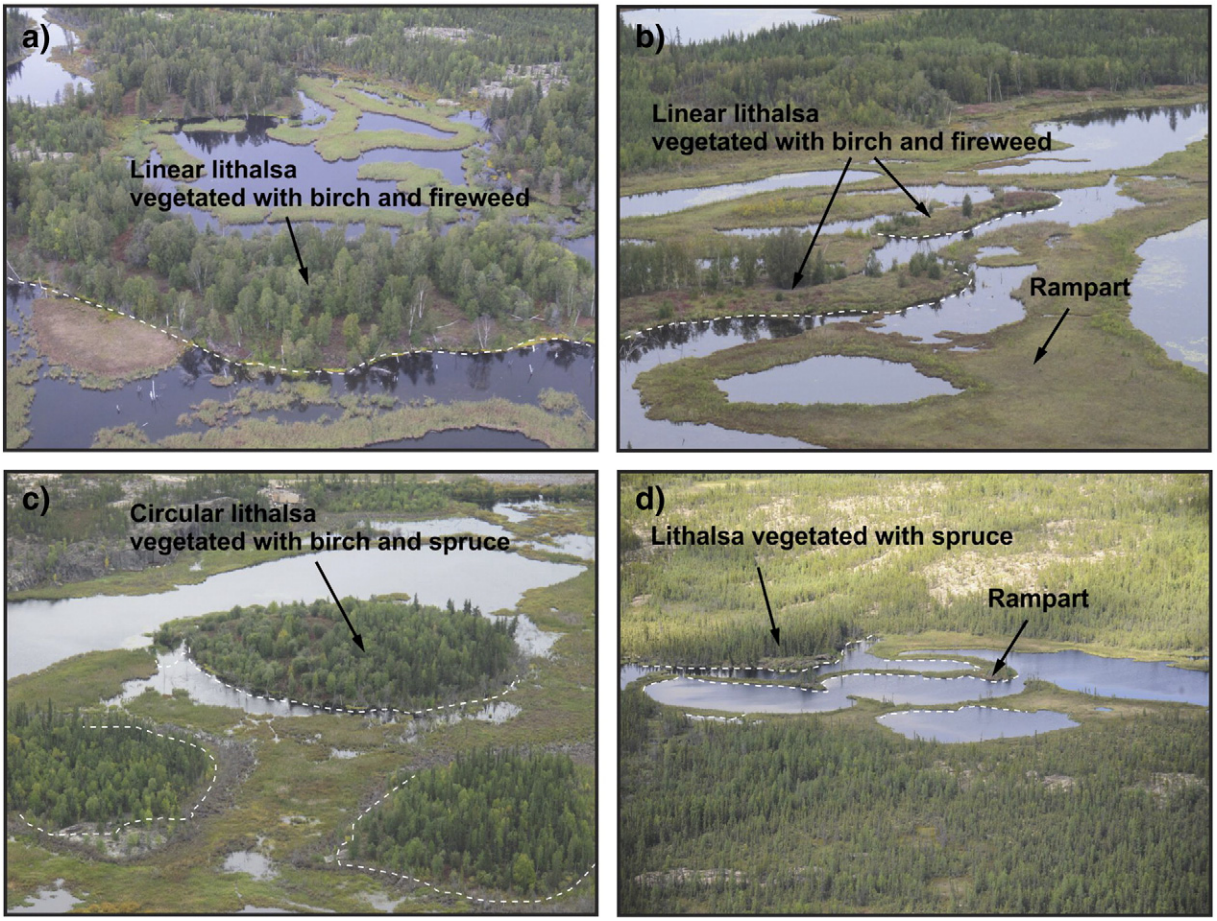

Fig. 9. Field photographs of lithalsas illustrating varying morphologies and vegetation cover, and an association with water bodies. a) Linear lithalsa at 62°40′29″N; 115°25′10″W; b) linear lithalsa and ramparts at 62°30′34″N; 114°54′52″W; c) circular lithalsa at 62°31′00″N; 114°51′00″W; d) lithalsa and ramparts at 62°27′44″N; 114°33′41″W.

Table 1
Land cover associated with lithalsas ($n = 175$) in the Great Slave Lowland. Land cover classification was derived from 10-m resolution SPOT-5 data. From Olthof et al. (2013).

Percent of lithalsas	Land cover name	Description
35	Deciduous — medium to high density	Deciduous, closed tree canopy (>40% cover), small coniferous-herb understory
35	Mixed — medium to high density	Mixed deciduous and coniferous tree canopy (>40%), small coniferous-herb understory
10	Coniferous — low to medium density	Coniferous low-medium density tree canopy (25–60%), shrub–lichen understory
7	Coniferous — medium density	Coniferous tree canopy (40–60%), lichen–shrub understory
6	Coniferous — high density	Coniferous tree canopy (>60%), lichen–shrub understory
4	Wetland/fen	Wetland vegetation, including fens, bogs, swamps, sloughs, and marshes
2	Spruce lichen bog	Wetland-type feature supporting wet lichen and conifer-treed bogs
1	Sparse coniferous-shrub cover	Sparse coniferous tree canopy (<25%), herb–shrub cover understory
0	Low vegetation and lichen (barren)	Grass and low lying herbaceous covers, lichen and sparse coniferous tree. Predominately non-vegetated and non-developed including exposed lands, rock, sediment, burned areas, rubble, or mines
0	Rock outcrop	Permanent with sparse vegetation that occurs on non-acidic and calcareous parent material in the high arctic
0	Bare/gravel/road	Bare ground-type materials such as soil, gravel, asphalt that are used to construct roads

ice segregation processes and rates may be comparable between lithalsas in differing environments.

Although lithalsas occur in a range of precipitation and ecological regimes including sub-arctic, forest tundra, steppe-larch forest and subtropical alpine, they all occur within sporadic to extensive discontinuous permafrost typically with a mean annual air temperature of about −4 °C, though ranging from −2 °C in Yukon to −7 °C in northern Quebec. Permafrost temperatures are warm and range between −0.2 °C and −0.8 °C. Active layer thicknesses are on the order of 90 to 200 cm and are notably thickest on the arid, unvegetated lithalsas of the Tso Kar Basin, India.

The sediment stratigraphy of contemporary lithalsas is very similar, typically with a cap of alluvial or lacustrine silt inter-layered or underlain by clay of glaciolacustrine, lacustrine or marine origin. Typical thicknesses of these fine-grained sediments are on the order of 10 m, and may be underlain by bedrock, fluvial gravels, or till.

The apparent age of all contemporary lithalsas is Holocene, and predominantly late Holocene. The lithalsas of the Great Slave Lake region span an age range from at least 8000 BP (i.e. the approximate age of terrestrial exposure at the highest elevations in the Great Slave Lowland) to potentially present-day, based upon historical lake level recession. Noting the relative abundance of lithalsas close to the present-day level of Great Slave Lake, many are likely less than 1000 years old, and may be forming at present. The apparent age of less than 700 years for the lithalsa described in this paper, which occurs at an elevation of about 10 m above the present lake level, is comparable in age to the estimated time of about 300 to 400 years for lithalsas to form elsewhere in Canada (Harris, 1993; An and Allard, 1995).

Vegetation succession and mature vegetation cover on contemporary lithalsas vary quite considerably, and are presumably reflective of the varied eco-climatic conditions in which they occur. Within the alpine regions of the Tso Kar Basin, India, and Akkol Valley, the Russian Altai Mountains, lithalsas are unvegetated or vegetated with steppe-grass cover, respectively, with minimal surface organic matter, owing to the comparatively arid environments of these regions. In contrast, in Canada, mature vegetation on most lithalsas includes succession towards forest cover with greater organic matter accumulations. In Quebec, succession trends towards black spruce and moss–lichen cover, whereas in Yukon mature vegetation cover trends towards white spruce, birch shrubs and moss, probably owing to more arid conditions in Yukon. In the Great Slave Lowland, mature vegetation cover typically includes deciduous forest cover of white birch, with white spruce and/or black spruce and an herb-dominated understory. Indeed, the generally tree-covered Lowland landscape is likely a primary reason why lithalsas have likely been previously undetected in this region, and the association of lithalsas with deciduous forest terrain appears unique.

Lastly, none of the lithalsas contain much, if any peat accumulation. Organic matter accumulation is typically on the order of about 10 cm, but appears to vary with the ecological succession (Harris, 1993) and dynamic state (Allard et al., 1996) of lithalsas.

Table 2
Examples of lithalsas in contemporary permafrost environments, and their climatic, stratigraphic, geomorphic and ecological settings. *MAAT* = mean annual air temperature; *MAGT* = mean annual ground temperature; *ppt* = annual precipitation; dis-pf = discontinuous permafrost.

Location; latitude/longitude; reference	Shape; height; width; vol ice content	Eco-climate; permafrost regime; *MAAT*; *ppt*; active layer thickness; *MAGT*	Stratigraphy; thickness	Geomorphic setting; age and formation requirement	Mature vegetation: trees; ground cover; organic matter thickness
Great Slave lowlands, NWT; 62°32′N 114°58′W; This Study	Circular, crescentic, linear; 0.5–8 m; 10–120 m; 50%	Sub-arctic; extensive dis-pf; −4.6 °C; 280 mm; 90–130 cm; ~−0.8 °C	Alluvial silt/lacustrine silt/glaciolacustrine clay/glaciofluvial/glacial/bedrock; 10–15 m	Stream valleys within (glacio) lacustrine terrain; Holocene (700 years)	Birch and white spruce or black spruce; herbs; 0 to 35 cm
Fox Lake, YT; 61°.10°N 135°23′W; Harris (1993, 1998)	Crescentic, circular; 2.2 m; 10–50 m; 60%	Sub-arctic; sporadic to extensive dis-pf; −2 °C; 220–360 mm; 130 cm −0.2 °C to −0.5 °C	Alluvial silt/lacustrine silt, colluvium; >5 m	Stream valleys within colluviated terrain; late Holocene (380 years)	White spruce and willow shrubs; moss; 0 to 50 cm
Eastern shore Hudson Bay QC; 56°37′N 76°13′W; Vallée and Payette (2007), Fortier and Aubé-Maurice (2008), Calmels et al. (2008a,b)	Circular; 2–3.4 m; 40–50 m 50 to 65%	Sub-arctic to forest tundra; sporadic to extensive dis-pf; ~−4.6 °C to −7 °C; 500–550 mm; 150–180 mm; −0.5 °C to −0.8 °C	Alluvial silt/marine/glacio-marine/glacio-fluvial/glacial/bedrock; 12 m	Stream valleys within (glacio) marine terrain; >3200 BP (400 years)	Black spruce; moss–lichen; 0 to >10 cm
Akkol Valley, Russian Altai Mountains; 49°50′N 88°E; Iwahana et al. (2012)	Linear; 3–6 m; 10–50 m; 52%	Steppe–larch forest; sporadic to extensive dis-pf; −4 °C to −6 °C; 360 mm; 120 cm; no data	Lacustrine or proglacial lake silts and silty clays; no data	Moraine terrace adjacent to ponds; 7650–5000 BP	Grass/unvegetated; <5 cm
Tso Kar Basin, Ladakha, India; 33°20 N 78°E; Wünnemann et al. (2008)	Circular, linear; 3–11 m; 2–400 m; 50%	Subtropical alpine; dis-pf; ~−4 °C; <90 mm; ~170–200 cm no data	Lacustrine silt and clay alternating with fluvial sand and gravel; no data	Lacustrine basin adjacent to lake; >4000 BP	Unvegetated salt crust; 0 cm

5.2. Controls on the distribution of lithalsas

As noted at the outset, Pissart (2000, 2002) predicted that probable locations of lithalsas in North America included the region north of Great Slave Lake, where the tree line adjoins the discontinuous permafrost limit. His hypothesis was based upon suggestions that lithalsas are restricted to the discontinuous permafrost zone, close to the treeline, where mean annual air temperature ranges from −4 °C to −6 °C and where the annual temperature of the warmest month is between +9 °C and +11.5 °C. He further suggested that the rarity of present-day and remnant lithalsas may be related, in part, to these specific climatic conditions needed to support them (Pissart, 2003).

Our findings confirm the existence of lithalsas in the Great Slave Lowland region, Northwest Territories, as predicted by Pissart (2000, 2002). Lithalsas are, in fact, widespread within the Lowland region, and this study, with comparisons to other contemporary lithalsa locations, provides further knowledge and constraints on their extent within discontinuous permafrost.

It is evident from our examination of contemporary lithalsas that three primary conditions; namely warm but widespread discontinuous permafrost, fine-grained sediment, and available groundwater supply, support the formation of lithalsas. The first condition is a comparatively warm permafrost ground thermal regime between 0 and −1 °C, but with extensive discontinuous permafrost. In particular, permafrost must be able to form within terrain that has a relatively thin (<10 cm) organic matter cover and, most notably, beyond the confines of peatlands (i.e. palsas and peat plateaus), as typically occur within sporadic discontinuous permafrost. For these reasons, regions with a mean annual temperature range between −4 °C and −6 °C typically satisfy these conditions. Notably, however, other climatic factors may play a role in lithalsa formation including limited total precipitation supporting localized aridity (Harris, 1993), and winter winds which may remove the snow cover that acts as an insulator inhibiting permafrost formation (Beaulieu and Allard, 2003). A warm permafrost ground thermal regime also appears essential to lithalsa formation, as it may promote ice lens formation by inhibiting rapid penetration of permafrost into the underlying substrate materials and maintain ground thermal conditions close to freezing, thus promoting cryosuction. In several contemporary settings, including Yukon and western Hudson Bay, the base of permafrost is located within 5 to 10 m of the surface (Harris, 1993; Allard et al., 1996).

Second, an underlying substrate of fine-grained frost susceptible material is a condition for the formation segregated ice lenses, and thus lithalsas. Most commonly, an underlying substrate of silt or clay of alluvial, lacustrine, glaciolacustrine, or marine origin, is associated with contemporary lithalsas. Significantly, this condition limits the distribution of lithalsas: more widespread occurrences are typically associated with former large lakes or marine basins, and small occurrences are associated with localized lake and pro-glacial lake environments. For these reasons, lithalsas are not found farther north in the Great Slave region, within till terrain, where they were predicted to occur based solely upon climatic controls (Pissart, 2000, 2002).

Third, an available groundwater supply is essential to lithalsa formation, as water availability likely affects lithalsa size, shape and cryostratigraphy via ground ice formation. Contemporary lithalsas are found in close proximity to surface water sources such as ponds, fens and streams, which represent talik (unfrozen ground) areas with renewable groundwater reserves. This groundwater acts to nourish ice-lens formation and promote heave in excess of the in-situ heave of localized pore water. Thus, lithalsas adjacent to water sources may grow several meters higher than the surrounding terrain. In complex terrain with bedrock exposures, peatlands, and variable sediment thicknesses, such as the Great Slave Lowland, lithalsas may take on a variety of morphological forms related to a spatially varying water supply. In more stratigraphically and topographically contiguous terrain, as in western Hudson Bay and the Tso Kar Basin, India, lithalsas tend to take on a more circular, symmetrical form owing, in part, to a more uniform water supply.

These three primary controls assist in understanding the distribution of lithalsas in permafrost environments, and may be used to assist in further predicting their occurrences in other areas. We hypothesize, for example, that lithalsas are more widespread in Canada than previously considered, and that both contemporary and remnant lithalsas may be found more broadly within the former glacial Lake McConnell basin, extending from Great Bear Lake to Lake Athabasca, and within other former glaciolacustrine basins. As noted at the outset, the recognition of these features is important as they represent potentially ice-rich, thaw-sensitive, and frost-susceptible terrain, which represents a hazard to expanding northern infrastructure.

The regional extent of lithalsas in the Great Slave Lowland may provide a unique opportunity to further examine the relation between lithalsas and present and past eco-climatic conditions. Notably, lithalsas in the region are most abundant near the present extent of Great Slave Lake, and decline in abundance with increasing elevation. Near the present shoreline of Great Slave Lake, lithalsas may, in fact, be presently forming, and an examination of the relation between lithalsa size and local ecological conditions could assist in testing this hypothesis. In addition, it is unclear if ramparts, noted in association with lithalsas represent remnant (thawed) lithalsas, or incipient forms with aggrading permafrost, or both — or if they are related to other processes entirely. Lastly, the cause for the spatial decline in lithalsas with elevation above Great Slave Lake in the Lowland is also unknown. This could be due to differing local conditions that support lithalsa formation, such as underlying sediment type and thickness, or topography and drainage that affect water supply. Alternatively, past climatic conditions may also affect the present distribution of lithalsas if, for example, lithalsas that formed at higher elevations subsequently decayed due to climatic or ecological changes. These issues are worthy of further consideration and would assist in understanding the past and present sensitivity of ice-rich terrain within discontinuous permafrost.

6. Conclusions

This study identifies ice-rich permafrost terrain features, known as lithalsas, within extensive discontinuous permafrost of the Great Slave Lowland, as previously predicted by Pissart (2000, 2002). These, and other contemporary lithalsas, require three conditions to form: warm but widespread discontinuous permafrost (not limited to organic peatland terrain), a substrate of fine-grained sediment frost susceptible sediment, and available groundwater supplied from nearby taliks. Where these conditions are suitably fulfilled, lithalsas may be widespread, and contain significant volumes of ground ice (up to 50% by volume) and grow to a height of 8 m and many hundreds of meters in length. Both contemporary and remnant lithalsas may be more common than previously recognized, as they may be widespread within former lacustrine, glaciolacustrine and marine basins with extensive discontinuous permafrost but obscured by forests or other vegetation cover. Recognition of contemporary and remnant lithalsas is significant as they represent potentially ice-rich, thaw-sensitive, and frost-susceptible terrain.

Acknowledgements

This work was conducted under the Great Slave — TRACS (Transportation Risk in the Arctic to Climatic Sensitivity) project and funded by the Climate Change Geoscience Program of Natural Resources Canada, with student financial support from the Northern Scientific Training Program, Aboriginal Affairs and Northern Development Canada. Helicopter logistics were provided by Trinity Helicopters, and financially supported by Polar Continental Shelf Project, Natural Resources Canada. This research was facilitated through co-operation with the Government of the Northwest Territories, Department of Transport

and Environment and Natural Resources, and with Aboriginal Affairs and Northern Development Canada. In particular, we thank Greg Cousineau, Steve Schwarz and Steve Kokelj for their ongoing support and collaboration in the Yellowknife area. Landcover classification was performed by Ian Olthof, Canada Center for Remote Sensing. Reviews by Caroline Duchesne, Peter Morse and Andrée Blais-Stevens are greatly appreciated. We further thank Benjamin Jones, an anonymous reviewer, and Takashi Oguchi for formal comments to improve the manuscript. The paper is the contribution number 20130119 of the Geological Survey of Canada.

References

Åckerman, H.J., Malmström, B., 1986. Permafrost mounds in the Abisko area, northern Sweden. Geogr. Ann. 68A, 155–165.
Åhman, R., 1976. The structure and morphology of minerogenic palsas in northern Norway. Biul. Peryglac. 26, 25–31.
Allard, M., Caron, S., Begin, Y., 1996. Climatic and ecological controls on ice segregation and thermokarst: the case history of a permafrost plateau in northern Québec. Permafr. Periglac. Process. 7, 207–227.
An, W., Allard, M., 1995. A mathematical approach to modeling palsa formation — insights on processes and growth-conditions. Cold Reg. Sci. Technol. 23, 231–244.
Beaulieu, N., Allard, M., 2003. The impact of climate change on an emerging coastline affected by discontinuous permafrost: Manitounuk Strait, northern Quebec. Can. J. Earth Sci. 40, 1393–1404.
Brown, R.J.E., 1973. Influence of climatic and terrain factors on ground temperature at three locations in the permafrost region of Canada. Proceedings of the Second International Conference on Permafrost, Yakutsk, USSR, North American Contribution. National Academy of Science, Washington, D.C., pp. 27–34.
Calmels, F., Allard, M., 2004. Ice segregation and gas distribution in permafrost using tomodensitometric analysis. Permafr. Periglac. Process. 15, 367–378.
Calmels, F., Allard, M., 2008. Segregated ice structures in various heaved permafrost landforms through CT Scan. Earth Surf. Process. Landforms 33, 209–225.
Calmels, F., Allard, M., Delisle, G., 2008a. Development and decay of a lithalsa in Northern Quebec: a geomorphological history. Geomorphology 97, 287–299.
Calmels, F., Delisle, G., Allard, M., 2008b. Internal structure and the thermal and hydrological regime of a typical lithalsa: significance for permafrost growth and decay. Can. J. Earth Sci. 45, 31–43.
Dionne, J.-C., 1978. Formes et phénomènes périglacaires en Jamésie, Québec subarctique. Géog. Phys. Quatern. 32, 187–247.
Dyke, A.S., Moore, A.J., Robertson, L., 2003. Deglaciation of North America. Geological Survey of Canada, Ottawa, Open File 1574. 32 maps, CD-ROM and 2 paper sheets.
Ecosystem Classification Group, 2008. Ecological Regions on the Northwest Territories: Taiga Shield.Department of Environment and Natural Resources, Government of the Northwest Territories (146 pp.).
Environment Canada, 2012. Climate Normals and Averages 1971–2000. Online data at http://www.climate.weatheroffice.ec.gc.ca/climate_normals/index_e.html.
Fortier, R., Aubé-Maurice, B., 2008. Fast permafrost degradation near Umiujaq in Nunavik (Canada) since 1957 assessed from time-lapse aerial and satellite photographs. In: Kane, D.L., Hinkel, K.M. (Eds.), Proceedings of Ninth International Conference on Permafrost, vol. 9, pp. 457–462.
Fortier, R., LeBlanc, A.-M., Allard, M., Buteau, S., Calmels, F., 2008. Internal structure and conditions of permafrost mounds at Umiujac in Nunavik, Canada, inferred from field investigations and electrical resistivity tomography. Can. J. Earth Sci. 45, 367–387.
Harris, S.A., 1993. Palsa-like mounds developed in a mineral substrate. In: Guangzhan, W. (Ed.), Sixth International Conference on Permafrost, Beijing, China, vol. 1. South China University of Technology Press, Guangzhou, pp. 238–243.
Harris, S.A., 1998. A genetic classification of the palsa-like mounds in Western Canada. Biul. Peryglac. 37, 115–130.
Heginbottom, J.A., Dubreuil, M.A., Harker, P.A., 1995. Canada — permafrost, National Atlas of Canada, 5th edition. National Atlas Information Service, Natural Resources Canada, MCR, p. 4177.
Hoeve, T.E., Seto, J.T.C., Hayley, D.P., 2004. Permafrost response following reconstruction of the Yellowknife Highway. International Conference on Cold Regions Engineering, Edmonton.
Iwahana, G., Fukui, K., Mikhailov, N., Ostanin, O., Fujii, Y., 2012. Internal structure of a lithalsa in the Akkol Valley, Russian Altai Mountains. Permafr. Periglac. Process. 23, 107–118.
Karunaratne, K.C., Kokelj, S.V., Burn, C.R., 2008. Near-surface permafrost conditions near Yellowknife, Northwest Territories, Canada. In: Kane, D.L., Hinkel, K.M. (Eds.), Proceedings Ninth International Conference on Permafrost, 9, pp. 907–912.
Lagarec, D., 1982. Cryogenic mounds as indicators of permafrost conditions, northern Quebec. Proceedings Fourth Canadian Permafrost Conference. NRC Press, Ottawa, pp. 43–48.
Lagerbäck, R., Rodhe, L., 1986. Pingos and palsas in northernmost Sweden — preliminary notes on recent investigations. Geogr. Ann. 68A, 149–154.
Lemmen, D.S., Duk-Rodkin, A., Bednarski, J.M., 1994. Late glacial drainage systems along the northwest margin of the Laurentide ice sheet. Quat. Sci. Rev. 13, 805–828.
Mackay, J.R., 1998. Pingo growth and collapse, Tuktoyaktuk Peninsula area, western Arctic Coast, Canada: a long-term field study. Géog. Phys. Quatern. 52, 271–323.
Mark, D.M., Church, M., 1977. On the misuse of regression in earth science. Math. Geol. 9, 63–74.
Nelson, F.E., Hinkel, K.M., Outcalt, S.I., 1992. Palsa-scale frost mounds. In: Dixon, J.C., Abrahams, A.D. (Eds.), Periglacial Geomorphology: Proceedings of the 22nd Annual Binghampton Symposium in Geomorphology. John Wiley & Sons, Chichester, pp. 305–325.
Oldenborger, G.A., 2012. Electrical resistivity surveys for permafrost terrain characterization along the Highway 3 corridor, Yellowknife, NWT. GSC Open File 7062.
Oldenborger, G.A., Stevens, C.W., Wolfe, S.A., 2012. Electrical geophysics for assessing permafrost conditions along highway infrastructure. Symposium on the Application of Geophysics for Engineering and Environmental Problems 2012 (6 pp.).
Olthof, I., Latifovic, R., Wolfe, S.A., Fraser, R., 2012. Medium-resolution land cover information from SPOT 4–5 across the subarctic treeline, Great Slave Region, NWT. 39th Annual Yellowknife Geoscience Forum, Program with Abstracts, Nov. 15–17, 2012.
Olthof, I., Latifovic, R., Pouliot, D., 2013. Medium resolution land cover map of Canada from SPOT 4/5 data. 34th Canadian Symposium on Remote Sensing Victoria, B.C. Remote Sensing: From Inspiration to Application, Program with Abstracts (August 27–29).
Payette, S., Seguin, M.-K., 1979. Les buttes minérales cryogènes dans les basses terres de la Revière aux Feuilles, Noveau-Québec. Géog. Phys. Quatern. 33, 339–356.
Pissart, A., 2000. Remnants of lithalsas of the Hautes Fagnes, Belgium: a summary of present-day knowledge. Permafr. Periglac. Process. 11, 327–355.
Pissart, A., 2002. Palsas, lithalsas and remnants of these periglacial mounds. A progress report. Prog. Phys. Geogr. 26, 605–621.
Pissart, A., 2003. The remnants of Younger Dryas lithalsas on the Hautes Fagnes plateau in Belgium and elsewhere in the world. Geomorphology 52, 5–38.
Pissart, A., 2010. The side growth of lithalsas: some comments on observations in Northern Quebec. Permafr. Periglac. Process. 21, 362–365.
Pissart, A., Harris, S., Prick, A., Vliet-Lanoe, V., 1998. La signification paleoclimatique des lithalsaes (palses minerals). Biul. Peryglac. 37, 141–152.
Pissart, A., Calmels, F., Westiaux, C., 2011. The potential lateral growth of lithalsas. Quat. Res. 75, 371–377.
Riseborough, D.E., Wolfe, S.A., Duchesne, C., 2012. Simplified climate statistics for permafrost modeling: Yellowknife case study. Proceedings of the 10th International Conference on Permafrost, Salekhard, Yamel-Nenets Autonomous District, Russia, pp. 335–340.
Ross, N., Harris, C., Brabham, P.J., Sheppard, T.H., 2011. Internal structure and geological context of ramparted depressions, Llanpumsaint, Wales. Permafr. Periglac. Process. 22, 2191–2305.
Seppälä, M., 1986. The origin of palsas. Geogr. Ann. 68A, 141–147.
Shan, J., Toth, C., 2008. Topographic Laser Ranging and Scanning Principles and Process. CRC Press (590 pp.).
Smith, D.G., 1994. Glacial Lake McConnell paleogeography, age, duration, and associate river deltas, Mackenzie River Basin, western Canada. Quat. Sci. Rev. 13, 829–843.
Stevens, C.W., Kerr, D.K., Wolfe, S.A., Eagles, S., 2012. Predictive surficial material and geology derived from LANDSAT 7, Yellowknife, NTS 85J, NWT. Geological Survey of Canada, Open File 7106, 1 CD-ROM.
Vallée, S., Payette, S., 2007. Collapse of permafrost mounds along a subarctic river over the last 100 years (Northern Quebec). Geomorphology 90, 162–170.
Westin, B., Zuidhoff, F.S., 2001. Ground thermal conditions in a frost-crack polygon, a palsa and a mineral palsa (lithalsa) in the discontinuous permafrost zone, Northern Sweden. Permafr. Periglac. Process. 12, 325–335.
Wünnemann, B., Reinhardt, C., Kotlia, B.S., Riedel, F., 2008. Observations on the relationship between lake formation, permafrost activity and lithalsa development during the last 20000 years in the Tso Kar Basin, Ladakh, India. Permafr. Periglac. Process. 19, 341–358.